Accepted Manuscript

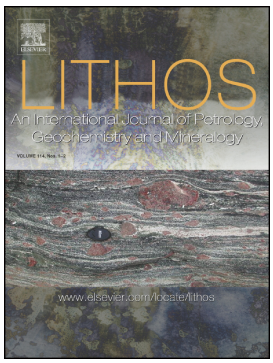

Combined garnet and zircon geochronology of the ultra-high temperature metamorphism: Constraints on the rise of the Orlica-Śnieżnik Dome, NE Bohemian Massif, SW Poland

Katarzyna Walczak, Robert Anczkiewicz, Jacek Szczepański, Daniela Rubatto, Jan Košler

PII: S0024-4937(17)30324-9
DOI: doi:10.1016/j.lithos.2017.09.013
Reference: LITHOS 4419

To appear in:

Received date: 18 September 2015
Accepted date: 19 September 2017

Please cite this article as: Katarzyna Walczak, Robert Anczkiewicz, Jacek Szczepański, Daniela Rubatto, Jan Košler , Combined garnet and zircon geochronology of the ultra-high temperature metamorphism: Constraints on the rise of the Orlica-Śnieżnik Dome, NE Bohemian Massif, SW Poland. The address for the corresponding author was captured as affiliation for all authors. Please check if appropriate. Lithos(2017), doi:10.1016/j.lithos.2017.09.013

Combined garnet and zircon geochronology of the ultra-high temperature metamorphism: Constraints on the rise of the Orlica-Śnieżnik Dome, NE Bohemian Massif, SW Poland.

Katarzyna Walczak[1,2], Robert Anczkiewicz[1], Jacek Szczepański[3], Daniela Rubatto[4,5], Jan Košler[6]

[1] *Institute of Geological Sciences, Polish Academy of Sciences, Kraków Research Centre, ul. Senacka 1, 31-002 Kraków, Poland*

[2] *Faculty of Geology, Geophysics and Environmental Protection, AGH–University of Science and Technology, Mickiewicza 30,30‑059 Kraków, Poland*

[3] *Institute of Geological Sciences, Wrocław University, Pl. M. Borna 9, 50-205 Wrocław, Poland*

[4] *Research School of Earth Sciences, Australian National University, Canberra 2601 ACT, Australia*

[5] *Institute of Geological Sciences, University of Bern, 3012 Bern, Switzerland*

[6] *Department of Earth Science and Centre for Geobiology, University of Bergen, Allegaten 41, N-5020 Bergen, Norway*

Corresponding author:

Katarzyna Walczak, Institute of Geological Sciences, Polish Academy of Sciences, Kraków Research Centre, ul. Senacka 1, 31-002 Kraków, Poland. E-mail: ndderwis@cyf-kr.edu.pl, Tel. +48 124221910, Fax: +48 124221609.

Abstract

Garnet and zircon geochronology combined with trace element partitioning and petrological studies provide tight constraints on evolution of the UHT-(U)HP terrain of the Orlica-Śnieżnik Dome (OSD) in the NE Bohemian massif. Lu-Hf dating of peritectic garnet from two mesocratic granulites constrained the time of its initial growth at 346.9±1.2 and 348.3±2.0 Ma recording peak 2.5 GPa pressure and 950 °C temperature. In situ, U-Pb SHRIMP dating of zircon from the same granulite gave a younger age of 341.9±3.4 Ma. Ti-in-zircon thermometry indicates crystallization at 810-860 °C pointing to zircon formation on the retrograde path. Lu partitioning between garnet rim and zircon suggest equilibrium growth and thus U-Pb zircon age constrain the terminal phase of garnet crystallization which lasted about 6 Ma.

All Sm-Nd garnet ages obtained for mesocratic and mafic granulites are identical and consistently younger than the corresponding Lu-Hf dates. They are interpreted as reflecting cooling of granulites through the Sm-Nd closure temperature at about 337 Ma.

The estimated PTt path documents the ca. 10 Ma evolution cycle of the OSD characterized by two distinct periods: (1) 347 - >342 Ma period corresponds to nearly isothermal decompression resulting from crustal scale folding and vertical extrusion of granulites, and (2) at >342-337 Ma which corresponds to a fast, nearly isobaric cooling.

Keywords: garnet and zircon geochronology, granulites, trace element partitioning, exhumation of UHP-UHT rocks, Bohemian Massif.

1. Introduction

In the Bohemian Massif of central Europe numerous occurrences of ultra-high-temperature (UHT) and high or ultra-high-pressure (UHP) granulites-eclogites offer an insight into geochemical and isotopic processes occurring at extreme conditions. One of the challenges in reconstructing the evolution of such rocks is their reliable dating and link between isotopic ages and the petrological record. U-Pb zircon dating is commonly the method of choice for dating high temperature metamorphism. This is due to the well acknowledged fact of U-Pb system in zircons being capable of quantitative retention of U and Pb even at extreme temperature conditions (Cherniak and Watson, 2003). Lu-Hf dating of garnets is a potential alternative for dating granulite facies rocks. As demonstrated by Anczkiewicz et al. (2007) under "dry", high temperature conditions Lu-Hf system in garnet may preserve the time of growth even in excess of 900 °C. Because of garnet involvement in most reactions used for constraining PT conditions the Lu-Hf garnet dating technique has a strong advantage over U-Pb method due to a relative ease of linking an isotopic age with metamorphic conditions. Zircon ages can be indirectly linked to metamorphic conditions using textures, mineral inclusions and trace element partitioning between garnet and zircon (e.g. Hermann and Rubatto, 2003; Kelly and Harley, 2005). Previous studies in Stary Gierałtów region of the Bohemian Massif in SW Poland suggested that the two geochronometers could behave very differently under such extreme conditions. On the basis of Lu-Hf garnet ages, Anczkiewicz et al. (2007) postulated the occurrence of a 380-390 Ma metamorphic episode that preceded the commonly accepted c. 340-350 Ma granulite facies event which had been earlier suggested on the basis of U-Pb zircon ages (Brueckner et al., 1991; Klemd and Bröcker, 1999; Turniak et al., 2000; Lange et al., 2002; Štípská et al., 2004; Lange et al., 2005; Schneider et al., 2006;; Bröcker et al., 2009).

In this study we investigate relative and absolute timing of garnet and zircon growth in the granulites using Lu-Hf garnet and U-Pb zircon dating combined with trace element

partitioning study. Additionally, we investigated the influence of UHT conditions on Lu-Hf isotope systematics in garnet. Finally, we provide tight time constraints on tectonic evolution of the OSD.

2. Regional geology

The Orlica-Śnieżnik Dome (OSD) is located on the northeastern margin of the Bohemian Massif (BM) in SW Poland (Fig. 1). The dome is mainly composed of amphibolite-grade, partly migmatized orthogneisses hosting mafic and mesocratic (U)HP-UHT rock inliers. Locally, orthogneisses alternate with belts of biotite to staurolite grade supracrustal rocks (Don et al., 1990). Orthogneisses are the dominant lithology and are subdivided into two main groups: porphyritic Śnieżnik gneisses and migmatitic Gierałtów gneisses. They reflect different strain facies of the same granitic precursor dated at 520 to 490 Ma (Oliver et al., 1993; Turniak et al., 2000; Kröner et al., 2001; Štípská et al., 2004; Lange et al., 2005) which intruded supracrustal sedimentary successions of Neoproteorozic to Ordovician age (Gunia, 1984; Gunia and Wierzchołowski, 1979; Gunia, 1989; Jastrzębski et al. 2010, Mazur et al., 2012; Mazur et al., 2015; Szczepański and Ilnicki, 2014). The whole sequence was metamorphosed and deformed during Variscan orogeny in response to collision of Saxo-Thuringia and Brunia terrains.

High and ultra-high pressure rocks within orthogneisses are represented by numerous, but relatively small, eclogite bodies. An exception is large body of mesocratic ultra-high temperature granulites with mafic inliers located in the Złote and Rychleby Mts (Fig. 1). Estimates of P-T conditions for (U)HP and UHT granulites cropping out at the Polish – Czech border suggest peak pressures of 2.5-3.5 GPa at 900-1100 ^{o}C (Bakun-Czubarow, 1992; Bröcker and Klemd, 1996; Klemd and Bröcker, 1999; Kryza et al., 1996). Štípská et al.

(2004) questioned the existence of an UHP event and claimed significantly lower peak pressure of 1.8 GPa at temperature of 900 ^{o}C. Slightly higher peak PT conditions of 20–22 kbar and ca. 900–920 ºC for Gierałtów granulites were postulated by Jastrzębski et al, (2015). Ferrero et al. (2015) documented nano-granite inclusions within garnets in mesocratic granulites from the Gierałtów area and estimated near UHP conditions of formation at 2.7 GPa and ≥ 875 ^{o}C. Mafic granulites bear a strong record of retrogression under amphibolite facies conditions at about 750 to 550 ^{o}C and 1.4 - 1.0 GPa pressure (Steltenpohl et al., 1993; Klemd and Bröcker, 1999; Štípská et al., 2004).

Numerous geochronometers have been applied in order to determine the timing of eclogite facies metamorphism in the OSD. The oldest ages range from 390-370 Ma and were obtained on (U)HP granulites and surrounding metapelites (Anczkiewicz et al., 2007; Gordon et al., 2005; Bröcker et al., 2009). The geological meaning of this episode still remains enigmatic and was lately questioned by Bröcker et al. (2009 and 2010). Most U-Pb zircon and Sm-Nd garnet ages group around 350-330 Ma and were interpreted as representing peak (U)HP metamorphism or as a temperature peak associated with partial melting (Brueckner et al., 1991; Klemd and Bröcker, 1999; Turniak et al., 2000; Lange et al., 2002; Štípská et al., 2004; Lange et al., *2*005; Schneider et al., 2006; Anczkiewicz et al., *2*007; Bröcker et al., 2009). Younger Ar-Ar ages spread from 350 to 320 Ma commonly are interpreted as cooling ages reflecting rapid uplift of the massif to shallow crustal levels (Steltenpohl et al., 1993; Maluski et al., 1995; Marheine et al., 2002; Lange et al., 2002; Gordon et al., 2005; Anczkiewicz et al., 2007; Chopin et al., 2012b).

3. Analytical methods

3.1. Electron microprobe major elements analyses

Major elements profiles in garnets and back-scattered electron (BSE) images of selected minerals were obtained with Cameca SX-100 in Electron Microprobe Laboratory at Warsaw University. Standard operating conditions were: acceleration voltage 15 kV, beam current 10 nA (biotite, feldspars), 20 nA (amphibole, pyroxene, garnet), beam diameter ~1 μm. Natural and synthetic silicate or oxide minerals were used for calibration. The raw data were corrected by ZAF procedure by use of PAP software provided by CAMECA.

3.2. Laser ablation ICP MS trace elements analyses

The trace elements analyses of garnet and zircon from mesocratic granulite (WPT4/1) were determined by laser ablation inductively coupled plasma mass spectrometer (LA ICP MS) at the Research School of Earth Sciences (RSES), Australian National University (ANU) using ArF excimer laser with 120 mJ output energy and 5 Hz repetition rate, coupled to an Agilent 7500 quadrupole ICP MS. Laser spot size was 40 or 53 μm for garnet and 24 or 32 μm for zircon analyses. NIST 612 synthetic glass was used as an external calibration, BCR standard was also monitored during zircon analyses. Ca (measured by EMP) or Si (stoichiometric value) content were used as internal standards for garnet and zircon. The trace elements analyses of garnet in mafic granulite (WPT4/2a) were carried out with New Wave UP 213 Laser Ablation System (Nd:YAG laser; 5 J/cm² energy density and 10 Hz repetition rate) coupled with Termo Finnigan Element 2 High Resolution ICP MS in the Bergen Geoanalytical Facility (BGF), University of Bergen. Spot size of 53 μm was used for all garnet analyses. NIST 612 glass was used as an external standard and Ca as measured by EMP was used for internal normalization. BCR-2 and NIST 610 glasses were monitored during analysis. The trace elements analyses of garnet in mesocratic granulite G05/3 were

carried out in Kraków Research Centre, Institute of Geological Sciences, Polish Academy of Sciences with RESOlution M-50 ArF excimer laser coupled with XSeriesII quadrupole ICPMS. Energy density of about 8 J/cm², beam size of 33 and 24 μm diameter and 5 Hz repetition rate were applied during the measurements. The results were normalized to NIST612 primary standard using recommended values of Jochum et al. (2011). Stoichiometric Si content was used as an internal standard. MPI-DING glasses served as secondary standards (Jochum et al. 2011).

3.3. Sm-Nd and Lu-Hf dating

Mineral and whole rock fractions were prepared by crushing, sieving, magnetic and heavy liquids separation. In the last step, garnet fractions were purified by hand-picking under a stereo-microscope. In order to verify the benefit of the time consuming hand-picking process, garnet fractions Grt3 were processed without hand-picking step. Representative splits of whole rock gravel size fractions were grounded to powder in an automated agate mortar. Sm-Nd and Lu-Hf dating was conducted in Kraków Research Centre, Institute of Geological Sciences, Polish Academy of Sciences. Isotopic ratios measurements were carried out using a Thermo Fisher MC-ICPMS *Neptune*. Details of sample digestion, ion exchange chromatography, mass spectrometric procedures follow modified procedures of Anczkiewicz et al. (2004) and Thirlwall and Anczkiewicz (2004). Normalizing ratios, decay constants and standards reproducibility are given in the footnote to Table 1. Age calculations were performed using ISOPLOT 3.0 (Ludwig, 2003) and age uncertainties are given at 2σ level.

3.4. U-Pb SHRIMP dating

Zircons separated from WPT4/1 mesocratic granulite were mounted in an epoxy resin and polished. Cathodoluminescence (CL) imaging was performed with Hitachi S2250-N at the Electron Microscope Unit, at the Research School of Earth Sciences (RSES), Australian National University (ANU) in Canberra. U-Pb isotopic analyses were performed using the Sensitive High Resolution Ion Microprobe (SHRIMP II) at RSES, ANU. Instrumental conditions and data acquisition for zircon analyses followed that of Williams (1998). The U-Pb isotopic ratios were corrected using TEMORA 1 reference zircon (Black et al., 2003). The data were corrected for common lead using measured $^{208}Pb/^{206}Pb$ (Williams, 1998). Common lead composition was assumed to be that of Broken Hill which approximates laboratory common lead background at the RSES laboratories. U-Th-Pb data processing was carried out with SQUID Excel macro of Ludwig (2000), and ISOPLOT 3.0 (Ludwig, 2003). Uncertainty of age estimate is given at 2σ level.

4. Phase equilibria calculations and PT path for the mesocratic granulite

We conducted PT estimates for mesocratic granulite WPT 4/1 for which we have the most complete data set. Samples petrography, photomicrographs (Fig. S1) and mineral chemistry (Table S1) used for the calculations are presented in the supplementary material. The equilibrium phase diagram was calculated in the system SiO_2–TiO_2–Al_2O_3–FeO–MgO–MnO–CaO–Na_2O–K_2O–H_2O (KNCFMASHT) using the Perple_X software (Connolly, 2005) with the internally consistent thermodynamic dataset of Holland and Powell (1998). Water content was established using loss on ignition (LOI) value which corresponds to the maximum H_2O content in the system (Halpin et al. 2007; Johnson and White, 2011). Rather small H_2O content estimated as 0.6 wt. % corresponds well with very minor amount of hydrous minerals (biotite and amphibole) found in the rock. We used the following non-ideal

solution models: garnet (White et al., 2007), orthopyroxene (Powell and Holland, 1999), clinopyroxene (Green et al., 2007), ternary feldspar (Benisek et al., 2010), muscovite (Coggon and Holland, 2002), amphibole (Massonne and Willner, 2008), ideal ilmenite-geikielite-pyrophanite solution and a hydrous silicate melt (Holland and Powell, 2001). We also performed calculations involving biotite (White et al.,2007) which show that the latter mineral occupies similar PT space as amphibole and do not influence topology and isopleths of HT and HP mineral assemblages.

The calculated P-T pseudosection (Fig. 2) documents a relatively wide stability field of the assemblage quartz + K-feldspar + phengitic muscovite + garnet + omphacite + zircon + rutile which in the analyzed P-T space is stable above 675 ^{o}C at 1.0 GPa and 1000 ^{o}C at 3.0 GPa. Generally, below this limit muscovite becomes unstable and partial melting starts. Under such conditions, mineral paragenesis are expected to contain one or two feldspars + quartz ± pyroxene ± garnet ± kyanite ± zircon ± Ti-rich phase (rutile or ilmenite depending on pressure). Our modeling indicates that cpx is stable almost in the considered PT range, except for a relatively small area below 750 ^{o}C and 1.2 GPa. The amount of cpx drastically drops to 1-2 vol% in PT conditions below 675 ^{o}C at 1.0 GPa and 1000 ^{o}C at 3.0 GPa (Fig. 2c) suggesting that during exhumation to medium PT conditions nearly all cpx may react out. The latter conclusion is in agreement with the absence of cpx in the mesocratic granulites.

In order to decipher PT evolution of the granulites we used chemical zonation patterns recorded by two garnet types with different zonation trends interpreted as: 1) relic growth zonation observed in larger crystals and 2) thermally relaxed profiles observed in vast majority of the remaining, smaller grains (Fig. S2). The cores of the first type of garnets (Grs32-33Py7-8Alm58-60Sps1) is consistent with crystallization above solidus in the ultra-high pressure field at P= 3.0-3.5 GPa and T ≥850-920 °C, in the coesite stability field (Fig. 2B, field I). Due to possible diffusional modification of the major element composition, T

estimates should be taken as minimum. The P estimate also requires some caution as coesite has so far not been found in these rocks. However, the presence of psuedormorphs after coesite was postulated by Bakun-Czubarow (1991, 1992) which later was questioned by Štípská et al., (2004). PT conditions recorded by the second type garnet (with core composition Grs28-30Py8-13Alm55-58Sps1) are just below the solidus. These garnets contain nanogranites in their cores indicating the onset of crystallization in the presence of melt. Around this rather narrow PT range the modeling predicts a reduction of cpx abundance from >10 vol.% above solidus to < 2 vol.% below solidus (Fig. 2B, field II). This change is accompanied by garnet increase by 2 – 4 vol.%, which is most likely a consequence of omphacite breakdown and garnet growth (Fig. 2C, D).

Rims of larger garnet grains with relic growth zonation have the same composition as edges of the diffused smaller garnet crystals (Grs26-27Py11-12Alm55-58Sps1, Fig. S2). Grossular and pyrope isopleths define relatively a narrow PT space between ca. 1.75 – 2.00 GPa at 900–950 ºC where this garnet composition is stable (Fig. 2B, field III). Consequently, metamorphic evolution of mesocratic granulites between points II and III suggests nearly isothermal decompression by ca. 1.0 to 1.5 GPa.

Further constraints on the PT history of the investigated granulite come from amphibole composition. Amphiboles in mesocratic granulite have Ca content between 1.87 – 1.90 a p.f.u. In the PT space isopleths corresponding to 1.9 Ca a p.f.u. content (not shown) trend along the upper margin of amphibole stability field corresponding to about 1.20 – 1.25 GPa and $\geq$ 690 – 760 ºC. (Fig. 2B, field IV). Importantly, the last stage of the documented PT path is outside cpx stability field, which agrees well with our petrographic observations. Thus, the second part of the PT path bounded by fields III and IV defines nearly isobaric cooling.

Sub-vertical zircon isopleths indicate that the main zircon growth event should be associated with the isobaric cooling portion of the reconstructed PT path. Changes in garnet volume during metamorphic evolution of the granulite are rather subtle and vary within a relatively narrow range from 12 – 16 vol% (Fig. 2D).

5. Trace elements composition in garnet

Unlike major elements which display diffused or some relic prograde growth zonation profiles, some trace elements show considerable rim-to-rim variations especially in the mesocratic granulites. The chondrite–normalized Rare Earth Elements (REE) patterns in all samples show a typical enrichment in heavy relatively to light REE. However, garnet in the mafic granulite is significantly poorer in REE and shows a smaller degree of HREE enrichment (Fig. 3a and Fig. 4), which most likely reflects differences in bulk rock composition and mineralogy. The mesocratic granulite garnet shows a moderate to strong HREE decrease from core to rim, particularly in sample G05/3, with Lu_N/Gd_N (N = normalized to chondrite) below unity in the rim (Fig. 3a). On the other hand, garnet in mafic granulite lacks significant zonation (Fig. 3a).

Rim-to-rim distribution profiles across garnet grains of key elements for our geochronological study (Nd, Sm, Lu and Hf or Zr) confirm the general observations depicted from the chondrite normalized plots (Fig. 4). Sm and Nd do not seem to show any regular rim-to-rim pattern and are nearly flat with random minor peaks or valleys. In contrast, Lu content in garnets from mesocratic granulites shows strong enrichment towards the core, forming a bell shape profile (Fig. 4a,b). The profiles reveal a small enrichment in HREE in the garnet core of the mafic granulite, however, the zonation trend is significantly less

pronounced and shows resorbed rims (Fig. 4c). Opposite to the HREE, Zr and Hf show gentle increase from core to rim (Fig. 4a,b,c).

6. Zircon internal structure and trace elements composition

Zircon grains separated from WPT4/1 mesocratic granulite are of two types: (1) light pink colour, isometric grains seldom forming soccer ball shape crystals (e.g. Fig. 5a: grains 1, 30, 41) and (2) colourless or light yellow, elongated grains with rounded edges (e.g. Fig. 5a: grains 15, 31, 35). Similarly to previous studies (Štípská et al., 2004; Lange et al., 2005; Bröcker et al., 2010) CL and BSE imaging revealed two distinct internal domains in zircons: (i) low CL emission and well-defined oscillatory zoning, typically located in cores (Fig. 5a: grains 8, 31, 45, 49), and (ii) very bright CL pattern with weak oscillatory (e.g. Fig. 5a; grains 8, 36 overgrowths) or radial sector zoning (e.g. Fig. 5a: grains 26, 30), typically forming overgrowths around cores. The overgrowths are volumetrically dominant in the isometric crystals. BSE imaging (Fig. 5b) additionally revealed frequent inclusions of tiny apatite, quartz and feldspar in the cores, whereas the overgrowths are virtually inclusions free.

The zircon cores have relatively high U (353-593 ppm) and Y (1320-1930 ppm) contents, high Th/U (0.45-0.74), and high Lu_N/Gd_N (21.0-26.5) reflecting enrichment in HREE relative to MREE (Fig. 3b).

The zircon overgrowths have relatively low U (37-135 ppm) and Y (35-95 ppm) content, variable Th/U (0.02-0.39 ppm), low Lu_N/Gd_N (0.92-1.43) ratios reflecting lack of enrichment in HREE with respect to MREE (Fig. 3b). Such REE patterns have been frequently observed in granulite facies zircons (Rubatto 2002, Herman and Rubatto, 2003; Harley et al., 2007). Both zircon core and overgrowth domains display negative Eu-anomalies, however, in the cores the anomaly is much stronger (average Eu/Eu* <0.1) than in the overgrowths (average

Eu/Eu* = 0.5). Content of Ti in the metamorphic overgrowths ranges from 19 to 30 ppm which corresponds to temperatures of 810-860°C (Ferry and Watson 2007).

7. Geochronology

7.1. Sm-Nd and Lu-Hf garnet dating

Summary of the Sm-Nd and Lu-Hf garnet dating results is presented in Table 1 and Fig. 6. In all three samples Sm/Nd ratios in garnet determined by the isotope dilution method are in agreement with LA ICPMS Sm/Nd analyses indicating high purity of the analysed fractions and negligible contamination by Nd bearing minerals (Table 1 and Fig.4).

Sm-Nd dating of the two mesocratic granulites resulted in good quality isochrons (MSWD < 1) defining 332.4 ± 5.2 and 337.6 ± 2.3 Ma ages for WPT4/1 and G05/3, respectively (Fig. 6a,c). Considerably better precision of the latter age is due to much larger Sm/Nd fractionation in G05/3 garnets and consequently much higher $^{147}Sm/^{144}Nd$ and $^{143}Nd/^{144}Nd$ ratios than in WPT4/1 garnets. Dating of mafic granulite was more problematic. All five fractions define a poor precision 346 ± 22 Ma date (MSWD =11). Closer inspection of the data shows that the excessive scatter is caused by the two whole rock analyses. When the whole-rock data are not considered and the calculations are based on clinopyroxene analyses, an age of 336.9 ± 6.0 Ma (MSWD = 0.41) is obtained which agrees with the results obtained for the mesocratic granulite (Fig. 6e). In the two mesocratic granulites, fractions Grt3, which were not purified by hand picking, do not show any handicap relatively to other garnet fractions and fit very well on the isochrons.

Although all three ages are identical within their uncertainties, the samples do show significant variations in isotopic systematics. The possible reason for the whole rock fraction

being unsuitable for initial ratio correction is the strong retrogression of the mafic granulite likely caused by infiltration by external fluids which could have modified the Nd isotopic composition of some matrix minerals, while the usually robust garnets remained a closed system. Alternatively, some unidentified inherited Nd is present in the matrix minerals, which shifted the whole rock analyses below the preferred isochron defined by garnet and clinopyroxene. Neither of the two explanations can be ruled out but the very good agreement of 336.9 ± 6.0 Ma grt-cpx isochron age with the ages obtained for the mesocratic granulites makes the use of clinopyroxene more credible.

The same mineral and whole rock fractions were used for Lu-Hf dating (Fig. 6b,d and f). The non-purified garnet fractions Grt3 in mesocratic granulites show a significant departure from the isochrons defined by the remaining data. Clearly, handpicking helped to improve the quality of Lu-Hf dating but had no detectable effect on Sm-Nd dating (see above). This is likely due to the fact, that Hf concentration in garnet is very low, and thus garnet is very sensitive to any contaminating Hf from inclusions. On the contrary, reasonably high Sm/Nd ratios are accompanied by extraordinarily high Nd content, which makes this system much less sensitive to contamination. Thus, fractions Grt3 were excluded from the final Lu-Hf age estimates which resulted in ages of 348.3 ± 2.0 Ma and 346.9 ± 1.2 Ma for the two mesocratic granulites WPT4/1 and G05/3, respectively (Fig. 6b,d). $^{176}Lu/^{177}Hf$ garnet ratios significantly vary between the two mesocratic granulites. This is the consequence of real differences between the two samples and not an analytical artifact (Table 1) as indicated by considerably higher HREE content in G05/03 garnets (Fig. 3a; Fig. 4b).

The Lu-Hf isochron for mafic granulite WPT4/2A defines an age of 343.2 ± 1.6 Ma (Fig. 6f). Unlike the Sm-Nd system, the whole rock and clinopyroxene fractions fall on the same isochron.

7.2. U-Pb SHRIMP zircon dating

U-Pb isotopic data for WPT4/1 mesocratic granulite are presented in Fig. 7 and in supplementary data Table S2. Apparent ages of zircon core spread over a wide range from c. 370 to 500 Ma, with some analyses being concordant, while others show various degree of discordance (Fig. 7). Mixing between different age component with post-crystallisation changes in the U-Pb systematics prior to 340 Ma event or a discordance due to common Pb carried in apatite inclusions (often present in zircon cores), are all possible explanation for observed data scatter.

The U-Pb dating results of 44 zircon overgrowths form a tight cluster and yield a weighted mean age of 341.9 ± 3.4 Ma (Fig. 7). One discordant analysis was excluded from age calculations.

8. Interpretation and discussion

8.1. Major and trace elements in garnet

Similarly to previous studies, we observed two different types of major element zonation trends in garnets, which are interpreted as: 1) relic growth zonation observed in larger crystals and 2) thermally relaxed profiles observed in vast majority of the remaining, smaller grains (Fig. S2). Trace element zonation in garnet is more pronounced. Sm and Nd show flat patterns in both types of granulites in all analyzed crystals (Fig. 4). Whether this is a result of high temperature equilibration or pristine growth feature is difficult to judge. Typically, the degree of Nd and Sm zonation is expected to be small (e.g. Kohn, 2009), but observations in some metapelites show that even under granulite facies temperature light REE zonation can

be significant especially in larger crystals, whereas smaller crystals tend to have flat profiles suggesting origin due to thermal relaxation (Anczkiewicz et al., 2012). Taking into account the very small size of the dated garnets and bearing in mind that the studied granulites are of magmatic protolith, we tentatively interpret the origin of Nd and Sm zonation as a result of thermal relaxation.

Heavy REE distribution in all studied garnets (Fig. 4) consistently shows enriched cores and depleted rims, resembling Rayleigh type zonation (Holister, 1966). The zonation is much stronger in the mesocratic (Fig. 4a,b) than in the mafic granulite. The difference is probably a consequence of different HREE partitioning between garnet and co-existing minerals in different bulk rock compositions. The reversed Lu zonation in some garnet rims (Fig. 4c) is likely related to resorption which locally is relatively strong, especially in the mafic granulite, where it is linked to the retrogressive amphibolitization event. Rayleigh zonation in garnet suggests that Lu profiles reflect the time of prograde garnet crystallization. Similarly Zr and Hf concentrations in all studied garnets increase gently from core to rim (Fig. 4) which is typical of growth zonation of incompatible elements (e.g. Yang and Rivers, 2002) and conforms with a common acceptance of very slow diffusivity of these elements in garnet (Van Orman et al., 2002; Bloch et al. 2015; Bloch and Ganguly 2015).

8.2. Relative timing of garnet and zircon growth

The inherited zircon cores have a well-developed oscillatory zoning, a high Th/U ratio and the trace element composition strongly enriched in heavy REE with a high HREE/MREE ratio (Fig. 3b) typical of zircon growing under magmatic conditions (e.g. Rubatto and Gebauer, 2000; Rubatto, 2002; Hoskin and Schaltegger 2003). Apparent U-Pb ages obtained for magmatic zircons show strong discordance and scatter from c. 370 Ma to c. 500 Ma (Fig.

7), preventing the determination of the precise age of the magmatic protolith. Admitting Pb loss as a major cause of age scatter, a minimum protolith age of ca. 500 Ma can be suggested which is in broad agreement with previous studies (Bröcker et al. 2010; Oliver et al. 1993; Turniak et al. 2000; and Kröner et al. 2001).

A 341.9 ± 3.4 Ma age of the zircon overgrowths comes within the range of Lu-Hf and Sm-Nd garnet dates which implies that zircon crystallization is a part of the same metamorphic history. The Ti-in-zircon thermometry returns temperature of 810–860 °C, well below peak temperatures of about 900 °C postulated in this and most previous studies (e.g. Štípská et al., 2004; Kryza et al., 1996; Bakun-Czubarow, 1992; Klemd and Bröcker, 1999). Such temperature range along with the weak oscillatory zoning within zircon overgrowths may suggest crystallization in the presence of melt. This is supported by the relatively high Th/U ratios (0.03-0.5) more typical of magmatic zircons. Rather high variability among Th/U ratios in the zircon overgrowths may be due to changing modal abundance of a Th-rich phase (e.g. monazite), for example due to dissolution in melt, during zircon crystallization.

The trace elements distribution between zircon and garnet in mesocratic granulite WPT4/1 (Fig. 3b, Fig. 8) provides an additional insight into relative timing of garnet and zircon growth. Garnet and metamorphic zircon qualitatively show very similar chondrite normalized REE patterns. The differences are confined to positive Ce anomaly present only in zircon and an overall higher REE content in garnet, particularly in its core (Fig. 3b). This is an indication that zircon likely grew in a bulk compositions depleted in M-HREE due to the presence of garnet. When the apparent partitioning garnet core–zircon and garnet rim–zircon are calculated (Fig. 8), the garnet core–zircon yield $D_{zirc/g.core}$ values around 0.1, far away from the proposed partitioning at UHT conditions under which $D_{zirc/g.rim}$ close to unity are expected (Harley et al., 2001, 2007; Rubatto and Hermann, 2007; Taylor et al., 2015) indicating that zircon did not crystallize in equilibrium with the garnet core, and thus likely later. For the

garnet rim composition, the $D_{zirc/g.rim}$ values are close to the expected value for the HREE from Er to Lu, whereas for REE larger than Er they fall increasingly below unity, i.e. below the preferred value (Harley et al. 2007; and Rubatto and Hermann 2007; Kotková and Harley, 2010). The $D_{zirc/g.rim}$ value is best constrained for HREE due to their higher abundance in both minerals. Additionally, diffusional homogenization of MREE in garnet as suggested by the flat zonation patterns (see above) will return wrong partitioning values for these elements. The exact value for the partitioning also depends on temperature and garnet composition (Rubatto and Hermann 2007; Van Westrenen and Draper, 2007; Taylor et al., 2015). Despite these uncertainties, the overall trend of $D_{zirc/g.rim}$ for HREE suggests that the garnet rim composition and metamorphic zircon likely crystallized in equilibrium. Our results are very similar to those of Kotková and Harley (2010) who studied similar UHT granulites and also interpreted their data as reflected equilibrium HREE partitioning between garnet rim and metamorphic zircon.

8.3. Garnet and zircon geochronology in the context of trace elements distribution

Preservation of strong zonation of HREE in mesocratic granulites along with the accepted view of slow diffusivity of Hf in garnet (Ganguly et al., 1998; Van Orman et al., 2002; Bloch et al., 2010) indicate that the Lu-Hf system recorded the time of garnet crystallization. Some caution, however, is required due to extremely high temperatures experienced by these rocks. Steep Lu zonation profiles do not necessarily exclude some degree of diffusional redistribution (partial diffusion would leave a similar record). Studies of trace element alone, although very helpful, are insufficient to make a firm conclusion in this respect (see also discussion in Anczkiewicz et al. 2012). Nevertheless, combined trace elements and

geochronological study of garnet and zircon allows building a coherent scenario that is outlined below.

The Lu-Hf garnet ages of 348.3 ± 2.0 and 346.9 ± 1.2 Ma obtained for the mesocratic granulites represent the oldest ages related to metamorphism. Garnet in the mafic granulite also yielded a precise but younger Lu-Hf age of 343.2 ± 1.6 Ma. Comparison of Lu concentrations determined by ID and *in situ* LA ICP MS methods shows that, in the absence of Lu-rich inclusions, the ID measurements recover the average Lu content in garnet (Fig. 4 and Table 1). The difference in Lu-Hf age between mesocratic and mafic granulite can be an apparent difference if garnet crystallization occurred over an extended period of time. This would lead to underestimating the age precision which represents purely analytical uncertainty. If our interpretation of HREE partitioning between garnet and zircon in mesocratic granulite is correct (i.e. zircon crystallized in equilibrium with garnet rim), we can constrain minimum duration of garnet growth in this sample. The 6.4±3.9 Ma duration of garnet growth is bracketed by the age difference between Lu-Hf garnet age (approximating the time of the core formation) and U-Pb zircon age (approximating the time of rim formation) and clearly indicates that precision our Lu-Hf ages does not take into account such a prolonged crystallization time.

However, we would be reluctant to ascribe the age difference between Lu-Hf garnet ages in mesocratic and mafic granulites fully to prolonged duration of garnet growth and overestimated age precision. Firstly, timing and duration of garnet growth in mafic protolith did not have to be the same. Secondly, a younger age for the garnet in the mafic granulite could be caused by post growth alterations such as garnet resorption which is more pronounced in amphibolitised mafic granulites and could shift the age towards a younger value (Kelly et al. 2011). Such garnet rim resorption would produce loss of incompatible Hf and back-diffusion of compatible Lu into garnet. The resorbed rims, however, are rather

narrow and the amount of back diffused Lu would not be particularly high. Although resorption probably influenced the Lu-Hf systematics, its effect on the final age was small, if not negligible. In our view, the Lu-Hf garnet age difference between mesocratic and mafic granulite could be related to a real difference in timing of growth in different bulk rock composition and/or, what at present seems more likely, to different Lu zonation styles in garnet. Lapen et al. (2003) proposed that in steeply zoned, enriched in Lu garnet core, the age can be biased towards early growth phase, whereas flatter profiles cause relative shift of ages towards volumetrically more significant rim. This confirms our observations showing that garnet from the mafic granulite, where core-to-rim Lu gradient is fairly small (Fig. 4c), records a younger age than garnet from the mesocratic granulite where core-to-rim Lu gradient is very steep (Fig. 4a,b). The garnet that preserves prograde Lu zoning is about 6±4 Ma older than the 341.9 ± 3.4 Ma metamorphic zircon that formed in equilibrium with the garnet rim (considering HREE distribution between garnet and zircon, see above). Based on zircon crystallization temperatures (c. 800 ^{o}C) lower than the peak metamorphic temperature (c. 900 ^{o}C), it is concluded that zircon formed during cooling of the mesocratic granulite. This is supported by thermodynamic modelling that shows increase of zircon abundance at the beginning of fast cooling (Fig. 2D).

All three Sm-Nd isochrons yield statistically identical ages of 332.4 ± 5.2, 337.6 ± 2.3 and 336.9 ± 6.0 Ma for WPT4/1, G05/3 and WPT4/2a granulites respectively (Fig. 6a,c and e; Table 1). Flat Nd and Sm patterns observed in all samples suggest diffusional re-equilibration, and together with the ages significantly younger than their Lu-Hf counterparts, the Sm-Nd ages are taken to constrain the time of cooling below the Sm-Nd closure in garnets. This is in line with experimental studies that postulate closure temperature of 700 ± 50 ^{o}C for Sm-Nd system in garnet (Tirone et al., 2005; van Orman et al., 2002), which is at least 150 ^{o}C below the peak metamorphic temperature in the studied rocks.

8.4. Timing of UHT granulite facies metamorphism and the rise of the Orlica-Śnieżnik Dome

One of the most debated issues in the studies of timing of the OSD metamorphism is the interpretation of an older group of ages suggesting the presence of pre-350 Ma metamorphism. Klemd and Bröcker (1999) reported 360 – 369 Ma Pb-Pb zircon ages (mafic granulite) interpreted as reflecting time of zircon crystallization from melt which took place before or during the early stages of high-grade metamorphism. Lange et al. (2005) linked the obtained 360 – 370 Ma U-Pb zircon SHRIMP ages (mafic granulite) to an early stage of HT metamorphism. Similar, 372 Ma Th-Pb monazite date reported for a gneiss from the Orlica Mountains (western part of the OSD) was interpreted as approximating the time of UHP metamorphism (Gordon et al., 2005). Anczkiewicz et al. (2007) obtained 373.8 ± 4.0 and 386.6 ± 4.9 Ma Lu-Hf garnet dates (for mafic and mesocratic granulite, respectively) which they linked to prograde path of UHT metamorphism and considered c. 344 Ma ages obtained by U-Pb zircon and Sm-Nd garnet dating as younger metamorphic event on the retrograde path. The data from this study allow addressing this discrepancy between zircon and garnet geochronology.

We dated mesocratic and mafic granulites from the same outcrop in Stary Gierałtów as sampled by Anczkiewicz et al. (2007) using the same analytical protocols. Our results did not reproduce c. 380 Ma garnet ages postulated in the earlier study. Figure 9 plots our results for the mesocratic granulite WPT4/1 together with the analyses from Anczkiewicz et al. (2007). This plot clearly shows reproducible garnet analyses in both studies, but also shows large difference in whole rock Hf isotope composition. In order to verify the accuracy of the Hf isotope composition measured by the latter authors, we performed additional whole rock analyses of sample 99-2. The results of Anczkiewicz et al. (2007) were well reproduced and

show the same low values of $^{176}Lu/^{177}Hf$ and $^{176}Hf/^{177}Hf$ isotope ratios. The inconsistency with the data presented in this study can be explained by the contribution from inherited Hf that strongly affected the whole rock ratios in sample 99-2. This inheritance is indicated by considerably higher Hf content and consequently lower $^{176}Lu/^{177}Hf$ accompanied by low $^{176}Hf/^{177}Hf$ ratios (Table 1; Fig. 9) in the Anczkiewicz et al. (2007) measurements. Thus, we treat Lu-Hf garnet dating of Anczkiewicz et al. (2007) as inaccurate due to inappropriate initial ratio correction. It seems rather likely, that old U-Th-Pb metamorphic zircon and monazite dates reported for the Orlica-Śnieżnik Dome suffered from similar problems and should be treated with caution.

Geochronological data obtained in this study along with thermodynamic and petrological estimates allow to place tighter constrains on early evolution of the Orlica-Śnieżnik Dome. The Lu-Hf ages obtained for garnets from the mesocratic granulites reflect early garnet growth which took place in the presence of melt as indicated by the presence of nanogranite inclusions in the garnet cores (Fig. S1c,d). Study of Ferrero et al. (2015) interpreted these garnets as peritectic and determined conditions of melt formation as c. 875 $^{\circ}$C at 2.7 GPa. Thus, these conditions correspond to the onset of garnet crystallization and are in a good agreement with metamorphic conditions recorded by type 2 garnets in this study. Consequently, Lu-Hf garnet ages of mesocratic granulites date near peak conditions at about 347 Ma (Fig. 2B, field III). The time of formation of garnet rim is indirectly determined by U-Pb dating of zircon that crystallized in equilibrium with garnet rim and gave 341.9±3.4 Ma age. Taking into account Ti thermometer, the temperature of zircon (and indirectly also garnet rim) formation was in the range of 810–860 °C indicating about 100 °C cooling from the metamorphic peak in about 5 Ma. The 343.2±1.6 Ma age of garnet from mafic granulites coincides with the termination of garnet growth in mesocratic granulite. Additionally, the latter dates provide a maximum age for the end of decompression which pre-dated zircon and

garnet rim crystallization in mesocratic granulite (Fig. 2B). Further 100 °C of cooling, down to c. 750-770 °C, was achieved by 337 Ma as documented by Sm-Nd garnet cooling ages (Fig. 2B). Importantly, a late stage of this isobaric cooling was very rapid as inferred on the basis of identical cooling ages recorded by isotopic systems with wide range of closure temperatures such as Sm-Nd in garnet and Ar-Ar in hornblende and micas.

The presented PTt path for the mesocratic granulite along with the remaining geochronogical data provide more precise constraints for the tectonic model of the OSD formation proposed by Štispka et al., (2004) and further developed by Chopin et al., (2012b). According to the latter model, the formation of the dome is a consequence of the collisional process involving subduction of the Saxothuringian continental crust beneath the Teplá-Barrandian terrane and subsequent collision of the Saxothuringian passive margin with the Brunovistulian terrane. Indentation of the Saxothuringia in front of the Brunovistulian terrane resulted in large-scale folding and exhumation of subducted crust. Exemplification of this process is the OSD which is a crustal scale antiform that started to rise by 347 Ma as indicated by dating results of initial garnet growth. Coeval melting lowered competence of the crust and increased its buoyancy which facilitated almost isothermal decompression from some 95 km depth (2.5 GPa pressure) to ca. 55 km (1.5 GPa pressure) within 6±4 Ma. Little cooling during decompression was likely caused by significant heat advection into thickened and hot crust as indicated by the presence of magmatic bodies such as Jawornik granitoids dated at 353 and 342 Ma (Skrzypek et al., 2014) or Bielice tonalite dated at 339 Ma (Parry et al., 1997). At this stage, the OSD granulites underwent fast exhumation at rate of ca. 7-8 mm/yr, which ended prior to 342 Ma and was followed by isobaric cooling. Initial cooling (about 100 °C in >5 Ma) accelerated around 337 Ma (see above) and was associated with little exhumation, not exceeding 1 mm/yr. Therefore, we correlate isobaric cooling with horizontal spreading of the

uplifted OSD rocks (Štipska et al., 2004; Chopin et al., 2012b), which explains high cooling rates with little exhumation taking place.

The proposed OSD cooling history outlined above differ from the model of Štipska et al. (2004) who proposed fast cooling and fast exhumation during decompression and slow cooling during horizontal spreading. Štipska et al. (2004) pointed out that cooling history they proposed contradicts numerical modelling results (Grasemann et al., 1998; Thompson et al., 1997) and differs significantly from the majority of studies conducted on UHP granulites in other regions. PTt path constrained in this study suggests that cooling pattern of the OSD UHP-UHT granulites, in general, follows the numerical modelling predictions and was no different from those observed in other metamorphic terrains (e.g. Duchêne et al., 1997; Romer and Rötzler, 2001).

9. Conclusions

We combined garnet and zircon geochronology with trace element geochemistry and petrology to constrain the evolution of granulites from the UHT-(U)HP terrain of the Orlica-Śnieżnik Dome. Our PT constraints suggest the presence of an UHP episode preserved in larger garnet crystals. Lu-Hf garnet dating of mesocratic granulites yielded 346.9±1.2 and 348.3±2.0 Ma ages while garnets from mafic granulite gave a 343.2 ± 1.6 Ma date. The age difference between the two types of granulites is attributed to REE zonation patterns and differences in bulk rock compositions.

Zircon growth in mesocratic granulite took place on a retrograde path at 341.9 ± 3.4 Ma which, according to Ti thermometry, corresponds to temperatures of 810-860 °C. Heavy REE partitioning study indicates equilibrium Lu partitioning between zircon and garnet rim at this

temperature. Thus, Lu-Hf ages along with U-Pb zircon date allow to place indirect constraints on duration of garnet growth in mesocratic granulite which lasted 6±4 Ma.

All Sm-Nd garnet ages, regardless of protolith, are identical and consistently younger than the corresponding Lu-Hf dates. They are interpreted as cooling of granulites through Sm-Nd closure temperature at about 337 Ma.

The obtained PTt path documents about 10 Ma evolution of the OSD granulites consisting of two distinct periods: 1) an earlier phase between ≤347 and 342 Ma of nearly isothermal decompression accompanied by fast exhumation followed by 2) slow exhumation during rapid, nearly isobaric cooling which lasted until 337 Ma. This simple two stage cooling history of the OSD region is similar to cooling histories commonly observed in ultra-high grade metamorphic terrains elsewhere.

Acknowledgments

This study was financed by Polish Ministry of Science and Higher Education grant No. N N307 057734 and financially supported by Polish Academy of Sciences, Institute of Geological Sciences grant No. HPT. R. Anczkiewicz acknowledges funding from internal IGS PAS grant. The research of J. Szczepański was funded by the University of Wrocław grant 1017/S/ING. We are grateful to the reviewers for their constructive comments and Sun-Lin Chung for editorial handling of the manuscript.

References

Anczkiewicz, R., Platt, J.P., Thirlwall, M.F., Wakabayashi, J., 2004. Franciscan subduction off to a slow start: evidence from high precision Lu–Hf garnet ages on high-grade blocks. Earth and Planetary Science Letters, 225, 147–161.

Anczkiewicz, R., Szczepański, J., Mazur, S., Storey, C., Crowley, Q., Villa, I.M., Thirlwall, M.F., Jeffries, T.E., 2007. Lu-Hf geochronology and trace element distribution in garnet: Implications for uplift and Exhumation of ultra-high pressure granulites in the Sudetes, SW Poland. Lithos, 95, 363-380.

Anczkiewicz, R., Thirlwall, M., Alard, O., Rogers, N.W., Clark, C., 2012. Diffusional homogenization of light REE in garnet from the Day Nui Con Voi Massif in N-Vietnam: Implications for Sm–Nd geochronology and timing of metamorphism in the Red River shear zone. Chemical Geology, 318-319, 16-30.

Bakun-Czubarow, N., 1991. Geodynamic significance of the Variscan HP eclogite–granulite series of the Złote Mountains in the Sudetes (SW Poland). Publications of the Institute of Geophysics, Polish Academy of Sciences, A – 19 (236), 215 – 244.

Bakun-Czubarow, N., 1992. Quartz pseudomorphos after coesite and quartz exoutions in eclogitic omphacites of the Złote Mountains in the Sudetes, SW Poland. Archiwum Mineralogiczne, 48, 3-25.

Benisek, A., Dachs, E., Kroll, H., 2010. A ternary feldspar-mixing model based on calorimetric data: development and application. Contributions to Mineralogy and Petrology, 160, 327–337.

Black, L.P., Kamo, S., Allen, CM, Aleinikoff, J.N., Davis, D.W., Korsch, R.J., Foudoulis, C., 2003. TEMORA 1: a new zircon standard for Phanerozoic U-Pb geochronology. Chemical Geology, 200, 155-170.

Bloch, E., Ganguly, J., Hervig, R., 2010. Diffusion kinetics of hafnium in garnet: experimental determination and geochronological implications. Goldschmidt Conference Abstracts 2010, Knoxville TN. p A97.

Bloch, E., Ganguly, J., Hervig, R., Cheng W.J., 2015. Lu-176-Hf-176 geochronology of garnet I: experimental determination of the diffusion kinetics of Lu3+ and Hf4+ in garnet, closure temperatures and geochronological implications. Contributions to Mineralogy and Petrology 169, DOI 10.1007/s00410-015-1109-8.

Bröcker, M., Klemd, R., 1996. Ultrahigh-pressure metamorphism in the Śnieżnik Mountains (Sudetes, Poland): P-T constraints and geological implications. Journal of Geology, 104: 417–433.

Bröcker, M., Klemd, R., Cosca, M., Brock, W., Larionov, A.N., Rodionov, N., 2009. The timing of eclogite facies metamorphism and migmatization in the Orlica-Snieznik complex, Bohemian Massif: constraints from a multimethod geochronological study. Journal of Metamorphic Geology, 27, 385-403.

Bröcker, M., Klemd, R., Kooijman, E., Berndt, J., Larinov, A., 2010. Zircon geochronology and trace element characteristics of eclogites and granulites from the Orlica-Śnieżnik complex, Bohemian Massif. Geological Magazine, 147, 339-362.

Brueckner, H.K., Medaris, L.G., Bakun-Czubarow, N., 1991. Nd and Sr ages and isotope patterns from Variscan eclogites of the eastern Bohemian Massif. Neues Jahrbuch für Mineralogie (Abhandlungen), 163, 169-193.

Cherniak, D., Watson, E.B., 2003. Diffusion in zircon. Reviews in Mineralogy and Geochemistry, 53, 113–143.

Chopin, F., Schulmann, K., Štípská, P., Martelat, J.E., Pitra., P., Lexa, O., & Petri, B., 2012. Microstructural and metamorphic evolution of a high pressure granitic orthogneiss during continental subduction (Orlica−Śnieżnik dome, Bohemian Massif). Journal of Metamorphic Geology, 30 (4), 347-376.

Chopin, F., Schulmann, K., Skrzypek, E., Dujardin, J.R., Lehmann, J., Martelat, J.E., Lexa, O., Corsini, M., Edel, J.B., Štípská, P., Pitra, P., 2012. Crustal influx, indentation, ductile thinning and gravity redistribution in a continental wedge: building a Moldanubian mantled gneiss dome with underthrust Saxothuringian material (European Variscan belt). Tectonics, 31 (1), doi:10.1029/2011TC002951.

Coggon, R., Holland, T.J.B., 2002. Mixing properties of phengitic micas and revised garnet-phengite thermobarometers. Journal of Metamorphic Geology, 20, 683–696.

Connolly, J.A.D., 2005. Computation of phase equilibria by linear programming; a tool for geodynamic modeling and its application to subduction zone decarbonation. Earth and Planetary Science Letters, 236, 524–541.

Don, J., Dumicz, M., Wojciechowska, I., Żelaźniewicz, A., 1990. Lithology and tectonics of the Orlica–Śnieżnik Dome, Sudetes; recent state of knowledge. Neues Jahrbuch für Geologie und Paläontologie, 179, 159–188.

Duchêne, S., Lardeaux, J.-M., Albarède, F., 1997. Exhumation of eclogites: insights from depth-time path analysis. Tectonophysics 280, 125–140.

Ferrero, S., Wunder, B., Walczak, K., O'Brien, P. J., Ziemann, M. A., 2015: Preserved near ultrahigh-pressure melt from continental crust subducted to mantle depths. Geology, 43 (5), 447-450.

Ferry, J., Watson, E., 2007. New thermodynamic models and revised calibrations for the Ti-in-zircon and Zr-in-rutile thermometers. Contributions to Mineralogy and Petrology, 154, 429-437.

Ganguly, J., Tirone, M., Herving, L.R., 1998. Diffusion Kinetics of Samarium and Neodymium in Garnet, and Method for Determining Cooling Rates of Rocks. Science, 281, 805-807.

Gordon, S.M., Schneider, D.A., Manecki, M., Holm, D.K., 2005. Exhumation and metamorphism of an ultrahigh-grade terrane: geochronometric investigations of Sudete Mountains (Bohemia), Poland and Czech Republic. Journal of the Geological Society of London, 162, 841-855.

Grasemann, B., Ratschbacher, L., Hacker, B.R., 1998. Exhumation of ultrahigh-pressure rocks: Thermal boundary conditions and cooling history. In: When Continents Collide: Geodynamics and Geochemistry of Ultra-high Pressure Rocks (eds Hacker, B. R. & Liou, J. G.), 117 – 139, Kluwer Academic Publishers.

Green, E., Holland, T., Powell, R., 2007. An order-disorder model for omphacitic pyroxenes in the system jadeite-diopside-hedenbergite-acmite, with applications to eclogitic rocks. American Mineralogist, 92, 1181–1189.

Gunia, T., 1984. Microflora of the vicinity of Nowy Waliszów (Krowiarki Mts., Central Sudetes). Geologia Sudetica, 19, 75–86.

Gunia, T., 1989. Acritarcha and microproblematica of the crystalline lime limestones from the vicinity of Romanowo Górne (Central Sudetes Mts, Krowiarki). Geologia Sudetica, 24, 101–137.

Gunia, T., Wierzchołowski, B., 1979. Microfossils from the quartzitic schists in vicinity of Goszów, Śnieżnik Kłodzki Massif, Central Sudetes. Geologia Sudetica, 14, 8-25.

Halpin, JA., White, RW., Clarke, GL., Kelsey, DE., 2007. The proterozoic P-T-t evolution of the Kemp Land coast, east Antarctica; Constraints from Si-saturated and Si-undersaturated metapelites. Journal of Petrology, 48, 1321-1349.

Harley, S.L., Kinny, P.D., Snape, I., Black, L.P., 2001. Zircon chemistry and the definition of events in Archaean granulite terrains. In: Cassidy, K.F., Dunphy, J.M., Van Kranendonk, M.J. (Eds.), Extended Abstracts of 4th International Archaean Symposium. AGSO Geoscience Australia Record 2001/37, Canberra, 511-513.

Harley, S.L., Kelly, N.M., Möller, A., 2007. Zircon Behaviour and the Thermal Histories of Mountain Chains. Elements, 3, 25 – 30.

Hermann, J., Rubatto, D., 2003. Relating zircon and monazite domains to garnet growth zones: age and duration of granulite facies metamorphism in the Val Malenco lower crust. Journal of Metamorphic Geology, 21, 833–852.

Holister, L.S., 1966. Garnet Zoning: An Interpretation Based on the Rayleigh Fractionation Model. Science, 154, 1647-1651.

Holland, T.J.B., Powell, R., 1998. An internally consistent thermodynamic data set for phases of petrological interest. Journal of Metamorphic Geology, 16, 309–343.

Holland, T.J.B., Powell, R., 2003. Activity-composition relations for phases in petrological calculations: an asymmetric multicomponent formulation. Contributions to Mineralogy and Petrology, 145, 492–501.

Hoskin, P.W.O., Schaltegger, U., 2003. The composition of zircon and igneous and metamorphic petrogenesis. In: Hanchar JM, Hoskin PWO (eds) Zircon, vol 53. Mineralogical Society of America, Washington, pp 27-62

Jastrzębski, M., Żelaźniewicz, A., Nowak, I., Murtezi, M. and Larionov, A.N., 2010. Protolith age and provenance of metasedimentary rocks in Variscan allochthon units: U–Pb SHRIMP zircon data from the Orlica–Śnieżnik Dome, West Sudetes. Geological Magazine, 147, 416–433.

Jochum, KP., Weis, U., Stoll, B., Kuzmin, D., Yang, QC., Raczek, I., Jacob, DE., Stracke, A., Birbaum, K., Frick, DA., Gunther, D., Enzweiler, J., 2011. Determination of Reference Values for NIST SRM 610-617 Glasses Following ISO Guidelines. Geostandards and Geoanalytical Research, 35 (4), 397-429.

Kelly, N., Harley, S., 2005. An integrated microtextural and chemical approach to zircon geochronology: refining the Archean history of the Napier Complex, east Antarctica. Contributions to Mineralogy and Petrology, 149, 57-84.

Kelly, E.D., Carlson, W.D., Connelly, J.N., 2011. Implications of garnet resorption for the Lu-Hf geochronometer: An example from the contact aureole of the Makhavinekh Lake Pluton, Labrador. Journal of Metamorphic Geology, 29 (8), 901–916.

Klemd, R., Bröcker, M., 1999. Fluid influence on mineral reactions in ultrahigh-pressure granulites: a case study in the Śnieżnik Mts (West Sudetes, Poland). Contributions to Mineralogy and Petrology, 136, 358–373.

Kohn, M.J., 2009. Models of garnet differential geochronology. Geochimica et Cosmochimica Acta, 73, 170 – 182.

Kotková, J., Harley, S.L., 2010. Anatexis during High-pressure Crustal Metamorphism: Evidence from Garnet Whole-rock REE Relationships and Zircon-Rutile Ti-Zr Thermometry in Leucogranulites from the Bohemian Massif. Journal of Petrology, 51, 1967-2001.

Kröner, A., Jaeckel, P., Hegner, E., Opletal, M., 2001. Single zircon ages and whole-rock Nd isotopic systematics of early Palaeozoic granitoid gneisses from the Czech and Polish Sudetes (Jizerské hory, Krkonoše and Orlica–Snežnik Complex). International Journal of Earth Sciences (Geol. Rundschau), 90, 304–324.

Kryza, R., Pin, C., Vielzeuf, D., 1996. High pressure granulites from the Sudetes (SW Poland): evidence of crustal subduction and collisional thickening in the Variscan Belt. Journal of Metamorphic Geology, 14, 531–546.

Lange, U., Bröcker, M., Mezger, K. and Don, J., 2002. Geochemistry and Rb-Sr geochronology of a ductile shear zone in the Orlica-Śnieżnik dome (West Sudetes, Poland). International Journal of Earth Sciences, 91, 1005–1016.

Lange, U., Bröcker, M., Armstrong, R., Trapp, E., Mezger, K., 2005. Sm–Nd and U–Pb dating of high-pressure granulites from the Złote and Rychleby Mts (Bohemian Massif, Poland and Czech Republic). Journal of Metamorphic Geology, 23, 133–145.

Lapen, T.J., Johnson, C.M., Baumgartner, L.P., Mahlen, N.J., Beard, B.L., Amato, J.M., 2003. Burial rates during prograde metamorphism of an ultra-high pressure terrane: an example from Lago di Cignana, Western Alps, Italy. Earth and Planetary Science Letters, 215, 57–72.

Ludwig, K.R., 2000. SQUID 1.00, A User's Manual, Berkeley Geochronology Center Special Publication, No. 2.

Ludwig, K.R., 2003. ISOPLOT: A Geochronological Toolkit for Microsoft Excel. Berkeley Geochronology Center Special Publication.

Maluski, H., Rajlich, P., Souček, J., 1995. Pre-Variscan, Variscan and early Alpine thermo-tectonic history of the north-eastern Bohemian Massif: Ar 40/Ar39Ar study. Geologische Rundschau, 84, 345–358.

Marheine, D., Kachlik, V., Maluski, H., Patocka, F., Żelaźniewicz, A., 2002. The 40Ar–39Ar ages from the West Sudetes (NE Bohemian Massif): constraints on the Variscan polyphase tectonothemal development. Palaeozoic Amalgamation of Central Europe. Special Publication, Geological Society of London, 133–135.

Massonne H.J., Willner A.P., 2008. Phase relations and dehydration behaviour of psammopelite and mid-ocean ridge basalt at very-low-grade to low-grade metamorphic conditions. European Journal of Mineralogy, 20, 867-879.

Mazur S., Aleksandrowski P., Kryza R., Oberc-Dziedzic T., 2006. The Variscan Orogen in Poland. Geological Quarterly, 50 (1), 89–118.

Mazur, S., Szczepański, J., Turniak, K., McNaughton, N.J., 2012. Location of the Rheic suture in the eastern Bohemian Massif: evidence from detrital zircon data. Terra Nova, 24, 199-206.

Mazur, S., Turniak, K., Szczepański, J., McNaughton, N.J., 2015. Vestiges of Saxothuringian crust in the Central Sudetes, Bohemian Massif: Zircon evidence of a recycled subducted slab provenance. Gondwana Research, 27, 825-839.

Oliver, G.J.H., Corfu, F., Krogh, T.E., 1993. U–Pb ages from SW Poland: evidence for a Caledonian suture zone between Baltica and Gondwana. Journal of the Geological Society, London, 150, 355–369.

Parry, M., Štípská, P., Schulmann, K., Hrouda, F., Ježek, J., Kröner, A., 1997. Tonalite sill emplacement at an oblique plate boundary: northeastern margin of the Bohemian Massif. Tectonophysics 280, 61–81.

Powell, R., Holland, T., 1999. Relating formulations of the thermodynamics of mineral solid solutions; activity modeling of pyroxenes, amphiboles, and micas. American Mineralogist, 84, 1–14.

Romer, R.L., Rötzler, J., 2001. P-T-t Evolution of Ultrahigh-Temperature Granulites from the Saxon Granulite Massif, Germany. Part II: Geochronology. Journal of Petrology, 42, 2015–2032.

Rubatto, D., Gebauer, D., 2000. Use of cathodoluminescence for U-Pb zircon dating by ion microprobe: Some examples from the Western Alps. In Cathodoluminescence in Geosciences (ed. M. Pagel et al.), 373-400, Springer.

Rubatto, D., 2002. Zircon trace element geochemistry: partitioning with garnet and the link between U–Pb ages and metamorphism. Chemical Geology, 184, 123–138.

Rubatto, D., Hermann, J., 2007. Experimental zircon/melt and zircon/garnet trace element partitioning and implications for the geochronology of crustal rocks. Chemical Geology, 241, 38–61.

Schneider, D.A., Zahniser, S.J., Glascock, J.M., Gordon, S.M., Manecki, M., 2006. Termochronology of the West Sudetes (Bohemian Massif): Rapid and repeated eduction in the eastern Variscides, Poland and Czech Republic. American Journal of Science, 306, 846–873.

Scherer, E., Munker, C., Mezger, K., 2001. Calibration of the lutetium-hafnium clock (vol 293, pg 683, 2001). Science, 293(5536): 1766-1766.

Skrzypek E., Lehmann J., Szczepański J., Anczkiewicz R., Štipská P., Schulmann K., Kröner A. and Białek D., 2014. Time-scale of deformation and intertectonic phases revealed by P-T-D-t relationships in the orogenic middle crust of the Orlica-Śnieżnik Dome, Polish/Czech Central Sudetes. Journal of Metamorphic Geology, 32, 981-1003.

Steltenpohl, M.G., Cymerman, Z., Krogh, E.J. & Kunk, M.J., 1993. Exhumation of eclogitized continental basement during Variscan lithospheric delamination and gravitational collapse, Sudety Mountains, Poland. Geology, 21, 1111–1114.

Štípská, P., Schulmann, K., Kröner, A., 2004. Vertical extrusion and middle crustal spreading of omphacite granulite: a model of syn-convergent exhumation (Bohemian Massif, Czech Republic), Journal of Metamorphic Geology, 22, 179-198.

Szczepański J., Ilnicki S., 2014. From Cadomian arc to Ordovician passive margin: geochemical records preserved in metasedimentary successions of the Orlica-Snieznik Dome in SW Poland. International Journal of Earth Sciences, 103, 627-647.

Taylor, R.J.M, Harley, S.L., Hinton, R.W., Elphick, S., Clark, C., Kelly, N.M., 2015. Experimental determination of REE partition coefficients between zircon, garnet and melt: A key to understanding high-T crustal processes. Journal of Metamorphic Geology, 33, 231-248.

Thirlwall, M.F., Anczkiewicz, R., 2004. Multidynamic isotope ratio analysis using MC-ICP-MS and the causes of secular drift in Hf, Nd and Pb isotope ratios. International Journal of Mass Spectrometry, 235, 59–81.

Thompson, A. B., Schulmann, K. & Jezek, J., 1997. Extrusion tectonics and elevation of lower crustal metamorphic rocks in convergent orogens. Geology, 25, 491–494.

Tirone, M., Ganguly, J., Dohmen, R., Langenhorst, F., Herving, R., Becker, H.W., 2005. Rare-earth diffusion kinetics in garnet: experimental studies and applications. Geochimica et Cosmochimica Acta, 69, 2385–2398.

Turniak, K., Mazur, S., Wysoczański, R., 2000. SHRIMP zircon geochronology and geochemistry of the Orlica–Śnieżnik gneisses (Variscan belt of Central Europe) and their tectonic implications. Geodinamica Acta, 13, 1–20.

Van Orman, J.A., Grove, T.L., Shimizu, N., Layne, G.D., 2002. Rare earth element diffusion in a natural pyrope single crystal at 2.8 GPa. Contributions to Mineralogy and Petrology, 142, 416–424.

Van Westrenen, W., Draper, D.S., 2007. Quantifying garnet-melt trace element partitioning using lattice-strain theory: New crystal-chemical and thermodynamic constraints. Contributions to Mineralogy and Petrology, 154, 717-730.

White, R.W., Powell, R., Holland, T.J.B., 2001. Calculation of partial melting equilibria in the system Na2O-CaO-K2O-FeO-MgO-Al2O3-SiO2-H2O (NCKFMASH): PARTIAL MELTING EQUILIBRIA IN NCKFMASH. Journal of Metamorphic Geology, 19, 139–153.

White, R.W., Powell, R., Holland, T.J.B., 2007. Progress relating to calculation of partial melting equilibria for metapelites. Journal of Metamorphic Geology, 25, 511–527.

Williams, I.S., 1998. U-Th-Pb geochronology by ion microprobe, in: McKibben, M.A., Shanks III, W.C., Ridley, W.I. (Eds.), Application of microanalytical techniques to

understanding mineralizing processes. Reviews in Economic Geology, Society of Economic Geologists, pp. 1-35.

Yang, P., Rivers, T., 2002. The origin of Mn and Y annuli in garnet and the thermal dependence of P in garnet and Y in apatite in calc–pelite and pelite, Gagnon terrane, western Labrador. Geological Materials Research, 4 (1), 1–35.

Figure Captions

Fig. 1. Geological sketch map of the Orlica-Śnieżnik Dome (OSD) with inset map of the Bohemian Massif. BU-Bardo Unit; ISF – Intra Sudetic Fault; KMC – Kłodzko Metamorphic Complex; MSNC – Moravo-Silesian Nappe Complex; NMU – Nové Město Unit; OPH – Sudetic ophiolite; OSD – Orlica–Śnieżnik Dome; SMB – Staré Město Belt; SZ- Skrzyna Zone,VG – Vrbno Group. Inset: EFZ – Elbe Fault Zone; MO – Moldanubian Zone; MS – Moravo–Silesian Zone; ST – Saxothuringian Zone. Modified after Mazur et al. (2006).

Fig. 2. Pressure–temperature pseudosection of mesocratic granulite sample WPT 4/1 for KNCFMASHT system. Bulk rock composition (in %wt) used for the calculations: SiO_2(66.548), Al_2O_3(15.045), FeO(6.693), MnO(0.101), MgO(0.865), CaO(3.661), Na_2O(3.429), K_2O(2.323) and TiO_2(0.694), melt in low pressure side, cpx out marks the line of cpx out mineral reaction. Cpx – clinopyroxene, Fsp – ternary feldsdpar, Mica – white mica, Gt – garnet, Melt – melt, Ilm – ilmenite, ky – kyanite, zrc – zirconium, ru – rutile, q – quartz. Phase assemblages are listed in supplementary data set.

(b) Same pseudosection showing garnet for xCa=molar Ca/(Ca+Mg+Fe), xFe=molar Fe/(Fe+Mg) and phengite composition isopleths; (c) cpx and melt volume %; (d) garnet and zircon volume %.

Fig. 3. (a) Chondrite-normalized rare earth elements patterns of garnets from mesocratic and mafic granulites from the Orlica-Śnieżnik Dome. (b) Chondrite-normalized REE patterns in both zircon domains and in garnets from WPT4/1 mesocratic granulite.

Fig. 4. Rim-to-rim zonation patterns of Lu, Zr/Hf, Nd and Sm in garnets from mesocratic (a,b), and mafic (c) granulites. Note the different vertical scale for different elements.

Fig. 5. Images of zircon crystals from WPT4/1 mesocratic granulite. (a) Cathodoluminescence images, circles indicate analysed spots, labels give analytical label (upper number) and $^{206}Pb/^{238}U$ age ± 1 sigma error in Ma (lower number). (b) Back-scattered electron images of zircons showing the inclusion-rich cores and the inclusion-free rims. See text for discussion.

Fig. 6. Sm-Nd and Lu-Hf isochron plots. Grt- garnet, wr – whole rock, cpx – clinopyroxene. Not-filled symbols represent data that were not included in the isochron calculation.

Fig. 7. U-Pb concordia diagram for zircon analyses from WPT4/1 mesocratic granulite.

Fig. 8. Zircon - garnet REE distribution coefficients D(zrc/grt) for middle and heavy REE in mesocratic granulite sample (WPT4/1) compared with previous experimental (Rubatto & Hermann, 2007) and empirical (Kotková & Harley, 2010; Harley et al., 2007) D(zrc/grt) values. Grt6 represents REE values for typical WPT4/1 mesocratic granulite garnet.

Fig. 9. Comparison of Lu-Hf data presented in this study (black squares) and in Anczkiewicz et al., 2007 (grey diamonds, dashed line). Age calculated for garnet and whole rock fractions from this article and garnet fractions from Anczkiewicz et al., 2007

Table 1. Summary of the Sm-Nd and Lu-Hf isotopic results.

Footnote to Table 1.

Abbreviations: Grt – garnet, WR – whole rock, Cpx – clinopyroxene. Uncertainties on Hf and Nd isotope ratio measurements are 2SE (standard errors) and refer to the last significant digits. $^{176}Lu/^{177}Hf$ errors are 0.5%, JMC475 yielded 0.282157±13 2SD (standard deviation) over the period of analyses. Mass bias correction to $^{179}Hf/^{177}Hf = 0.7325$. Decay constant $\lambda_{176Lu} = 1.865x10^{-11}$ yr^{-1} (Scherer et al., 2001). $^{147}Sm/^{144}Nd$ errors are 0.3%, reproducibility of JNdi-1 Nd standard over whole period of analyses $^{143}Nd/^{144}Nd = 0.512097±13$ (2SD). Decay constant $\lambda_{147Sm}= 6.54x10^{-12}$ yr^{-1}. Age calculations conducted using Isoplot v. 4.15. Where *in run* errors were smaller than the external precision, propagated errors were used for age calculations. Age uncertainties are 2σ.

SUPPLEMENTARY MATERIALS:

Samples petrography.

Fig. S1. Photomicrographs (a-c) and BSE images (d) of analysed samples: (a) typical mesocratic granulite (WPT4/1) texture, (b) typical mafic granulite (WPT4/2A) texture with primary clinopyroxene, (c) cluster of nanogranite in garnet core (mesocratic granulite WPT4/1), (d) BSE image of negative garnet shape nanogranite in mesocratic granulite (WPT4/1) garnet.

Fig. S2. Rim-to-rim major elements zonation patterns in garnets from: (a-c) WPT4/1 mesocratic granulite zonation profiles used for phase diagram calculations (see text for details). #Fe=Fe/(Fe+Mg). (d) G05/3 mesocratic granulite and (e) WPT4/2A mafic granulite.

Table S1. Microprobe analyses of garnets from the studied granulites.

Table S.2. Summary of the U-Pb zircon analyses for mesocratic granulite WPT4/1 zircons.

Fig. 1

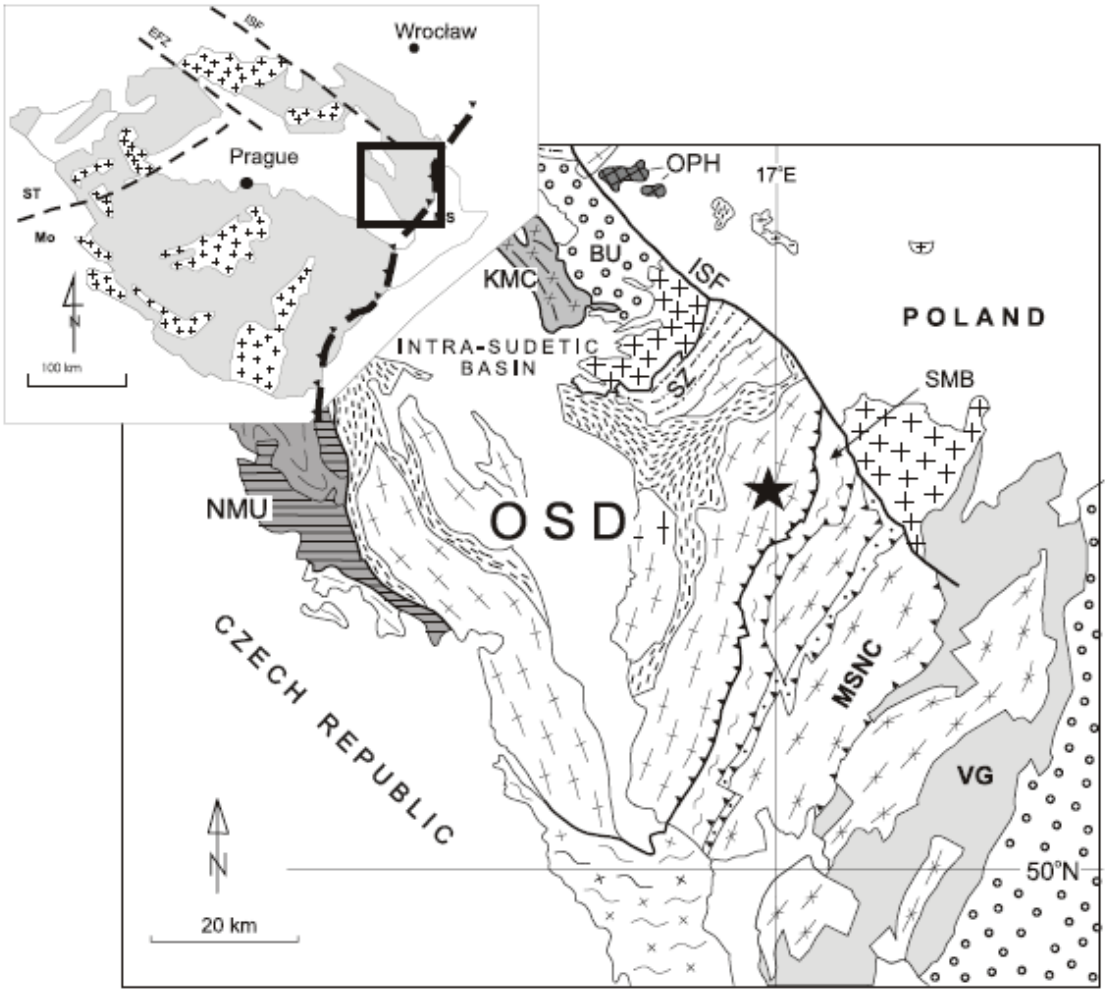

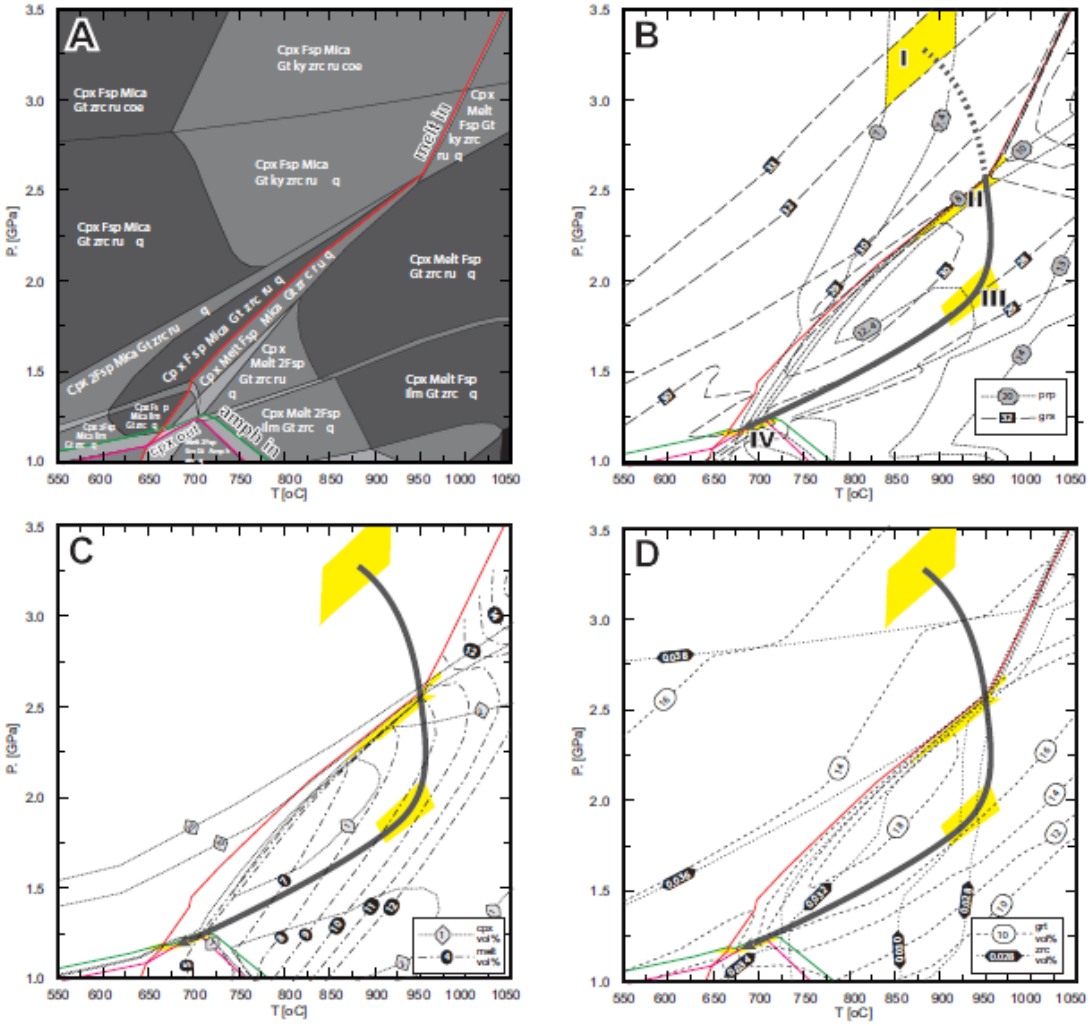

Figure 2

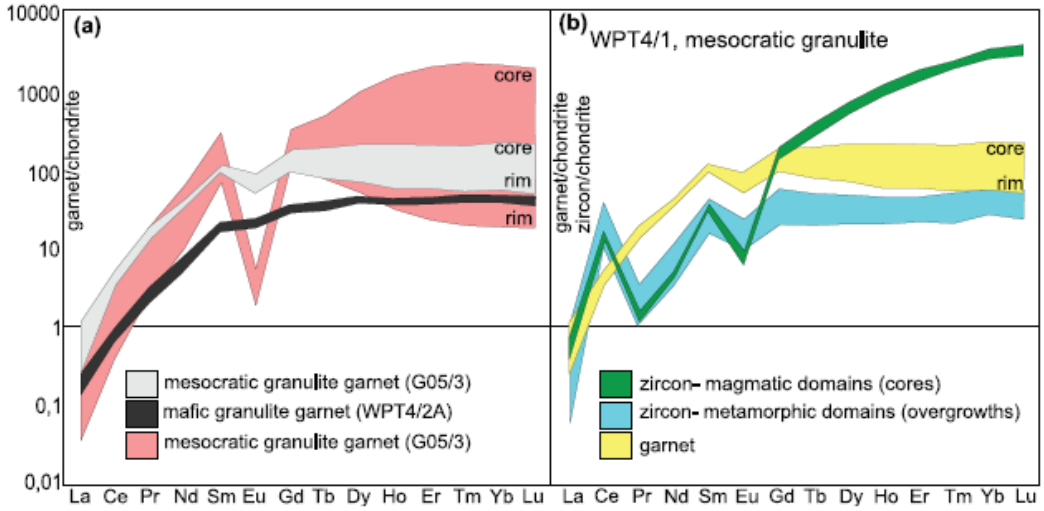

Figure 3

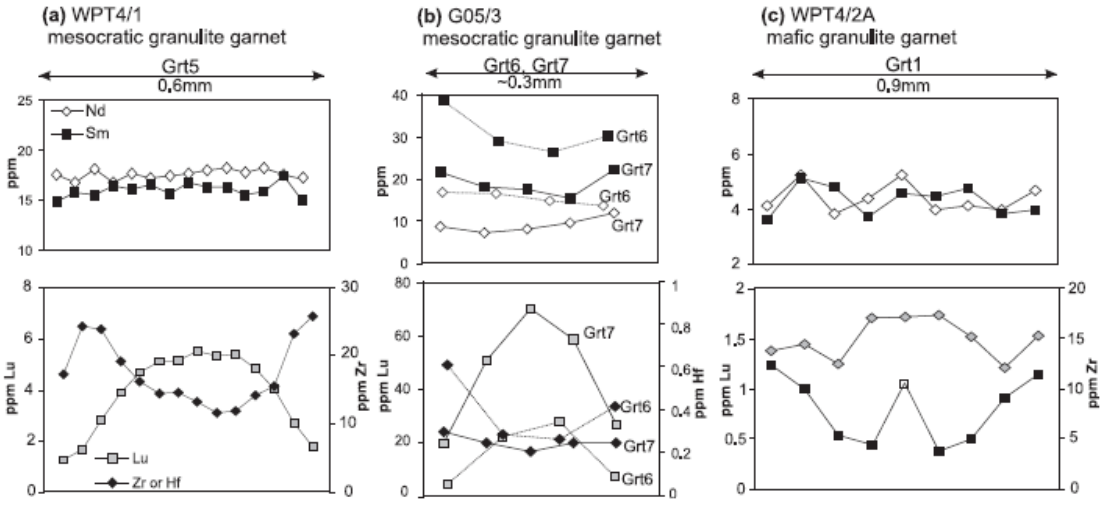

Figure 4

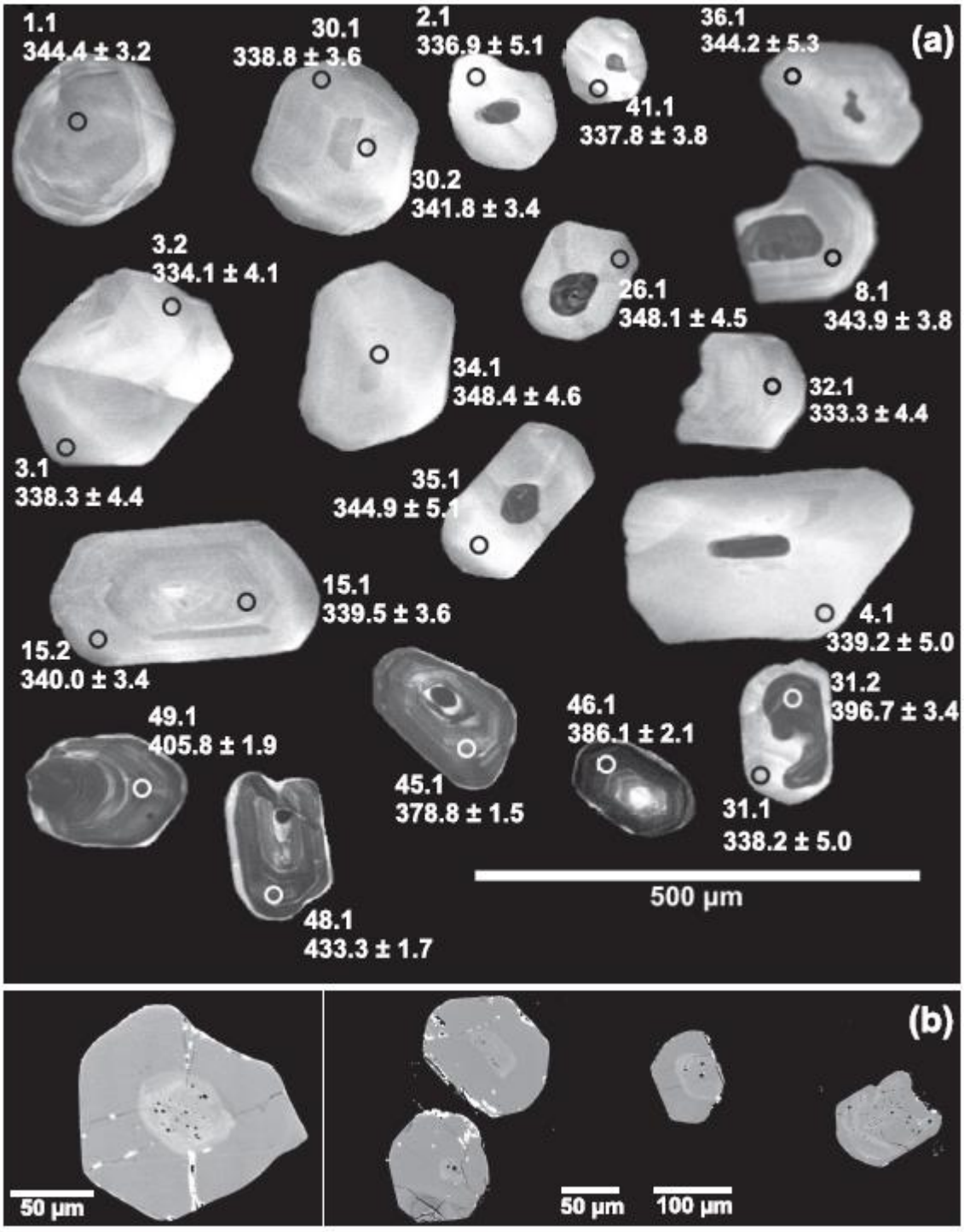
1.1
344.4 ± 3.2
30.1
338.8 ± 3.6
2.1
336.9 ± 5.1
36.1
344.2 ± 5.3
(a)
41.1
337.8 ± 3.8
30.2
341.8 ± 3.4
3.2
334.1 ± 4.1
26.1
348.1 ± 4.5
8.1
343.9 ± 3.8
34.1
348.4 ± 4.6
32.1
333.3 ± 4.4
3.1
338.3 ± 4.4
35.1
344.9 ± 5.1
15.1
339.5 ± 3.6
4.1
339.2 ± 5.0
15.2
340.0 ± 3.4
31.2
396.7 ± 3.4
49.1
405.8 ± 1.9
46.1
386.1 ± 2.1
45.1
378.8 ± 1.5
31.1
338.2 ± 5.0
500 µm
48.1
433.3 ± 1.7
50 µm
(b)
50 µm
100 µm

Figure 5

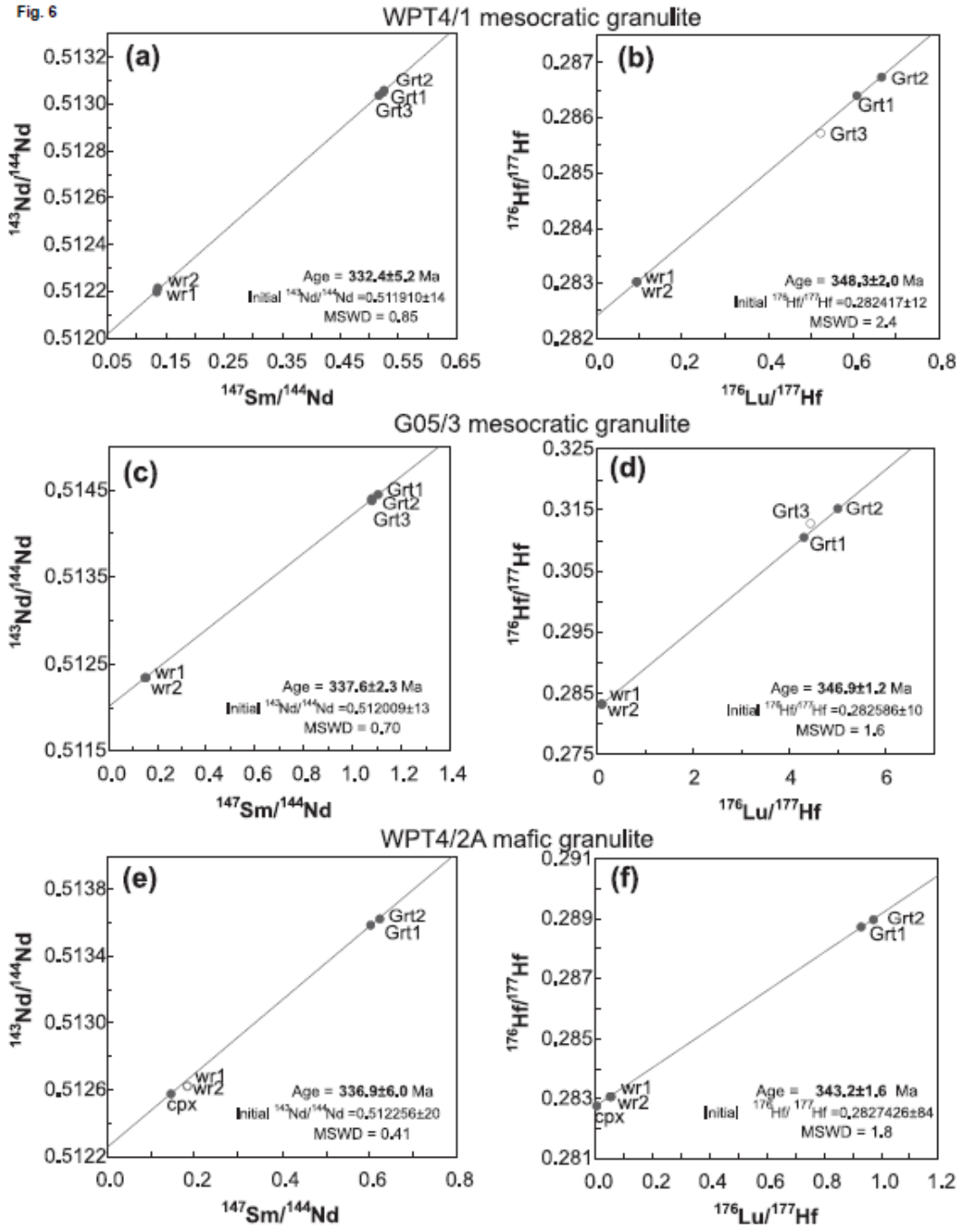

Figure 6

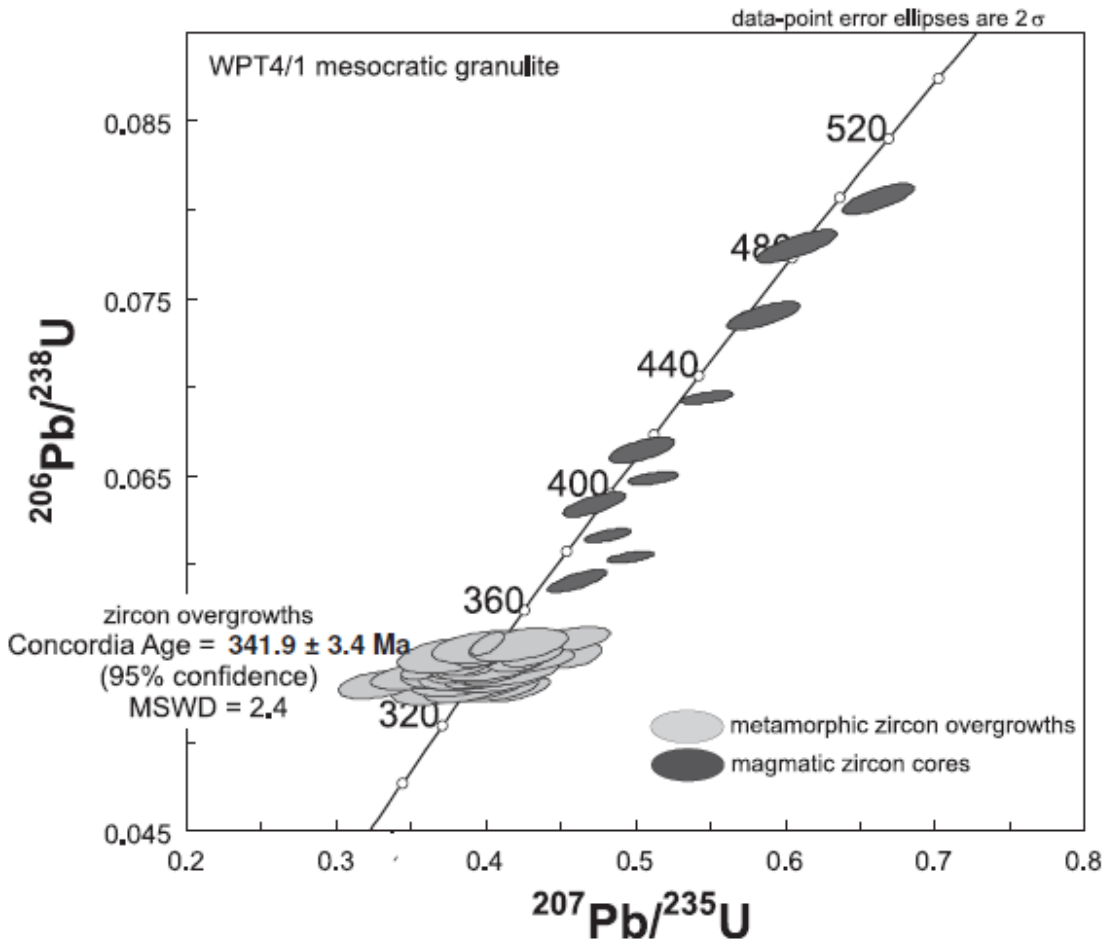

Figure 7

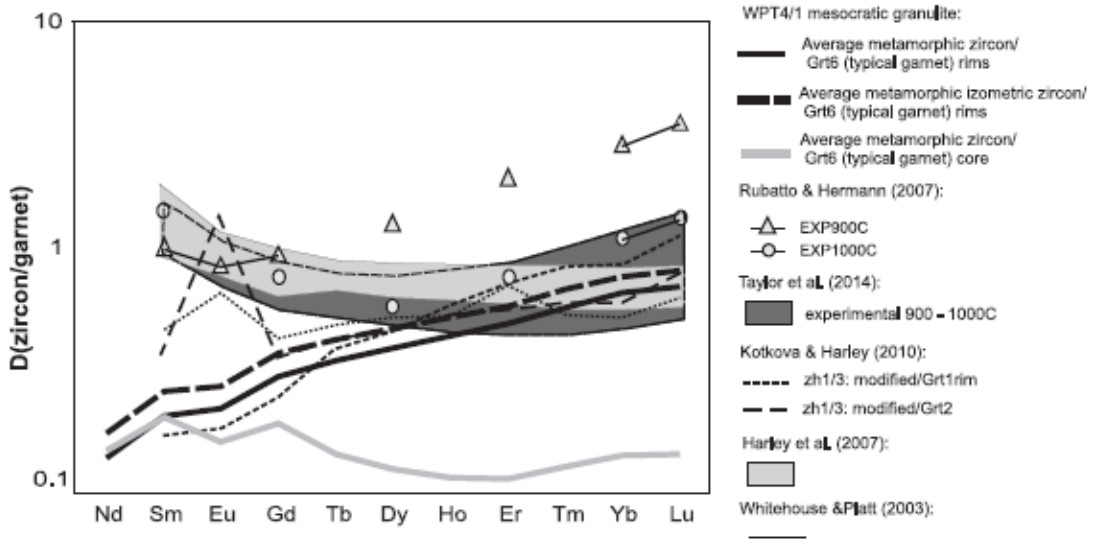

Figure 8

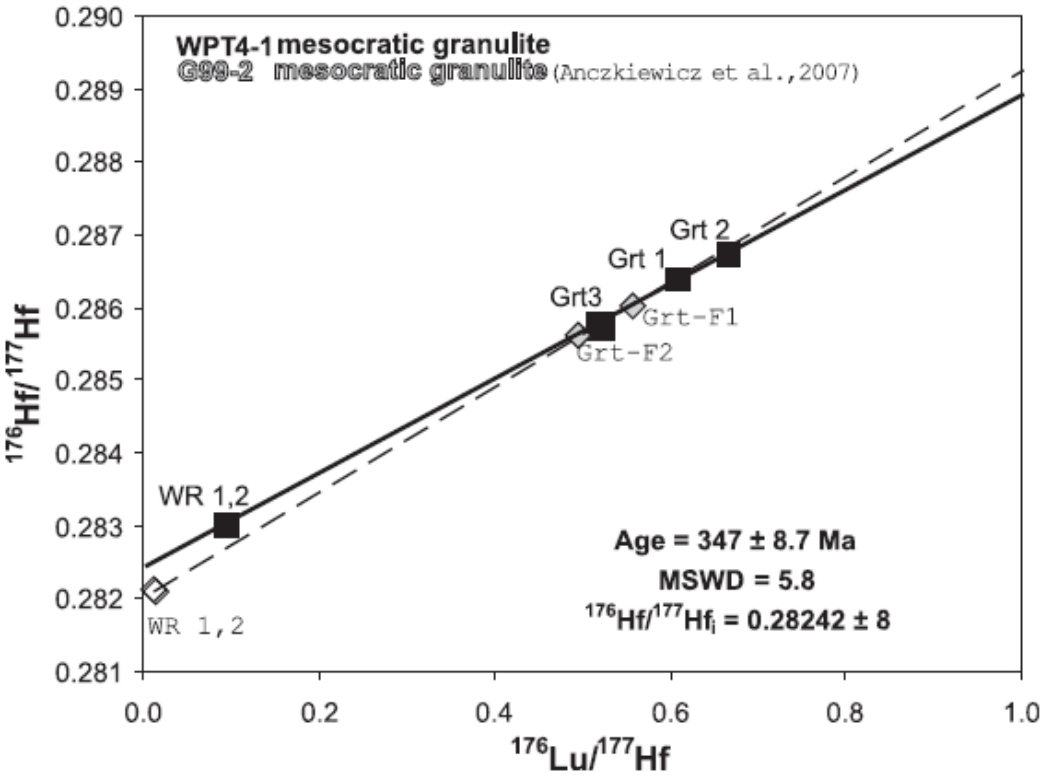

Figure 9

Table 1. Summary of the Sm-Nd and Lu-Hf isotopic results.

Label	Sample wt [g]	**Sm** [ppm]	**Nd** [ppm]	^{147}**Sm/**^{144}**Nd**	^{143}**Nd**/^{144}**Nd**	**Age [Ma]**	**Lu** (ppm)	**Hf** (ppm)	^{176}**Lu/**^{177}**Hf**	^{176}**Hf/**^{177}**Hf**	**Age [Ma]**
Felsic granulite WPT4/1; Stary Gierałtów											
Grt 1	0.04041	17.737	20.446	0.5245	0.513049±9	**332.4 ± 5.2**	2.962	0.689	0.6082	0.286399±5	**348.3 ± 2.0**
Grt 2	0.04054	18.127	20.848	0.5257	0.513057±5		3.022	0.643	0.6655	0.286734±8	
Grt 3	0.04077	17.951	20.967	0.5177	0.513037±6		*3.002*	*0.617*	*0.5201*	*0.285755±5*	
WR 1	0.08074	7.855	35.074	0.1354	0.512197±7		0.728	1.090	0.0944	0.283028±6	
WR 2	0.10206	7.822	34.725	0.1362	0.512215±6		0.732	1.106	0.0936	0.283030±4	
Mafic granulite WPT4/2a; Stary Gierałtów											
Grt 1	0.05120	4.260	4.281	0.6018	0.513587±8	**336.9 ± 6.0**	1.263	0.192	0.9297	0.288733±16	**343.2 ± 1.6**
Grt 2	0.05214	4.264	4.139	0.6230	0.513627±7		1.286	0.187	0.9723	0.288968±18	
cpx	0.05045	2.750	11.435	0.1454	0.512577±8		0.035	1.832	0.0027	0.282767±5	
WR 1	*0.11217*	*3.759*	*12.253*	*0.1855*	*0.512626±8*	*351.8 ± 5.3*	0.588	1.570	0.0530	0.283078±7	
WR 2	*0.10200*	*3.785*	*12.358*	*0.1851*	*0.512620±7*		0.596	1.620	0.0520	0.283070±5	
Felsic granulite G05/3;											
Grt 1	0.05101	49.967	27.314	1.1065	0.514454±7	**337.6 ± 2.3**	25.661	0.846	4.3131	0.310500±5	**346.9 ± 1.2**
Grt 2	0.05115	48.962	27.415	1.0802	0.514405±8		26.499	0.753	5.0065	0.315173±7	
Grt 3	0.05101	49.075	27.483	1.0800	0.514389±6		*24.652*	*0.790*	*4.4517*	*0.312529±9*	
WR 1	0.08183	4.608	18.296	0.1522	0.512342±8		0.763	1.063	0.1015	0.283240±3	

WR 2	0.0802	4.790	19.575	0.1479	0.512339±9		0.752	1.148	0.0926	0.283191±7	
Felsic granulite G99-2, Anczkiewicz et al., 2007											
Grt-F1	0.0264	19.710	24.744	0.4814	0.512942±8	**320.5 ± 3.0**	2.699	0.690	0.5582	0.286027±11	**386.6 ± *4.9***
Grt-F2	0.0375	23.277	26.780	0.5254	0.513037±7		2.987	0.852	0.4963	0.285610±319	
WR 1	0.0965	8.016	35.224	0.1376	0.512217±8				0.0127	0.282130±4	
WR 2	0.0778	8.338	36.753	0.1371	0.512224±8		0.830	7.581	0.0155	0.282100±10	

Grt – garnet, WR – whole rock, cpx – clinopiroxene. Age errors were calculated using Isoplot (Ludwig, 2003), errors are 95% confidence level.

Errors are 2SE.Age errors were calculated using Isoplot (Ludwig, 2003) and are 95% confidence level. Age errors and initial ratios errors are propagated for daily standard reproducibility. $^{147}Sm/^{144}Nd$ errors are 0.3%. Reproducibility of JNdi-1 Nd standard was $^{143}Nd/^{144}Nd$ = 0.512097±13(2SD) over whole period of analyses. $^{176}Lu/^{177}Hf$ errors are 0.5%. Reproducibility of JMC475 Hf standard was $^{176}Hf/^{177}Hf$ = 0.282157±(2SD) over whole period of analyses. Decay constant $\lambda_{176Lu} = 1{,}865 \times 10^{-11}$ rok^{-1} (Scherer et al., 2001) was used for Lu-Hf age calculations.

Highlights

Garnet rim/zircon HREE partitioning indicates equilibrium growth on a retrograde path
Lu-Hf and U-Pb geochronology constrains 5 Ma duration of peritectic garnet growth
PTt path documents two stage, c. 10 Ma cooling/exhumation cycle of UHP-UHT granulites